Cancer Chemother Pharmacol (1994) 34: 280 – 286

Cancer Chemotherapy and Pharmacology

The quinoline-3-carboxamide Linomide inhibits angiogenesis in vivo

P. Borgström[1], I.P. Torres Filho[1], P. Vajkoczy[2], K. Strandgården[2], J. Polaçek[2], B. Hartley-Asp[2]

[1] La Jolla Institute for Experimental Medicine, La Jolla, CA 92037, USA
[2] Kabi Pharmacia Therapeutics, S-223 63 Lund, Sweden

Received: 19 November 1993 / Accepted: 9 February 1994

Abstract. Linomide (Roquinimex) has antitumor activity when given in vivo (but not when applied in vitro) that has been attributed to immune host mechanisms. Recent studies, however, suggest that Linomide may also possess antiangiogenic properties. The aim of the present study was to evaluate the antiangiogenic effect of Linomide using an intravital microscopic technique. Syngeneic pancreatic islets were isolated and implanted into the dorsal skinfold chamber of Syrian golden hamsters. This model allows detailed repeated in vivo observations and quantitative analysis of revascularization of pancreatic islet grafts. The neovascularization process of the islets is a highly reproducible phenomenon that is completed within about 2 weeks, resulting in a microvascular network very similar to that of islets in situ. The plasma concentration profile of Linomide following a single oral dose of the compound was determined. The elimination of Linomide was fast, the half-life being 2.6 ± 0.2 h. Due to the short half-life, the hamsters were given Linomide twice a day. One group of animals ($n = 9$) was force-fed Linomide (100 mg/kg per day) from the day of implantation throughout the 2-week observation period, and the results were compared with those obtained in a nontreated control group ($n = 7$). At days 6, 10, and 14 after implantation, the neo-vasculature of the islets was examined. In the control group, $91\% \pm 4\%$ (mean $\pm$SEM) of the islets showed the first signs of angiogenesis at day 6, whereas in the Linomide-treated group the corresponding value was $48\% \pm 12\%$. At days 10 and 14, the "take-rate" in the control group increased to $94\% \pm 3\%$ for day 0 and to $94\% \pm 4\%$ ($n = 6$) for day 14, whereas in the treated group the corresponding take-rate was $67\% \pm 11\%$ and $72\% \pm 12\%$, respectively. The functional capillary density in the control group at days 6, 10, and 14 was 223 ± 17, 348 ± 29, and 495 ± 29 cm^{-1}, respectively, and that in the Linomide treated group was 91 ± 28, 181 ± 43, and 229 ± 47 cm^{-1}, respectively. These results demonstrate that Linomide suppresses the neovascularization of the islet grafts by both delaying the onset of and reducing the percentage of islets displaying angiogenesis as well as by decreasing the rate of proliferation of capillary endothelium of the revascularized islets.

Key words: Linomide – Angiogenesis – Antiangiogenic

Correspondence to: P. Borgström, La Jolla Institute for Experimental Medicine, 11077 North Torrey Pines Road, La Jolla, CA 92037, USA

Introduction

Linomide (Roquinimex), a quinoline-3-carboxamide, has been shown to possess anti-tumor activity when given in vivo [10, 11, 13, 14] but not when applied in vitro [13]. Such data suggest that the effects of Linomide are host-mediated, and several studies have focused on the effects of Linomide on immune cell functions. Those studies have revealed that in mice, Linomide enhances natural killer (NK)-cell activity [15], inhibits autoimmunity in MRL/1 mice [32], and enhances the proliferation of mitogen-stimulated T-cells [17]. When given systemically to rats, Linomide enhances the delayed-type hypersensitivity reaction to bacterial antigens [30], enhances mitogen-stimulated proliferation of T-cells [31], and inhibits the growth of a wide variety of Dunning prostate tumors [13] and dimethylbenzanthracene-induced mammary tumors [31]. However, in rats, Linomide treatment does not enhance either NK-cell numbers or NK-cell-induced cytotoxicity 28 days after treatment [13], nor does treatment of rats with anti-asialo GM_1, which suppresses NK cytotoxicity, interfere with Linomide antitumor effect [13]. Furthermore, Linomide has been shown to evoke antitumor effects in nude rats [13]. These data are suggestive of Linomide having other than direct immunomodulating properties. In a recent study [34] it was demonstrated that in a newly developed in vivo assay of angiogenesis [24], Linomide had dose-dependent antiangiogenic activity in rats. In the same study, in vitro assays using human umbilical-vein endothelial cells indicated that Linomide had cytostatic but not cytotoxic activity and that Linomide affected both chemotactic migration and invasion of human umbilical-vein endothelial cells.

To elucidate in more detail the proposed antiangiogenic properties of Linomide we decided to implement a newly developed intravital microscopic model using the hamster skin-fold preparation with syngeneically transplanted islets of Langerhans [19]. This model allows repeated intravital microscopic analysis and quantitative evaluation of the revascularization process of pancreatic islet isografts.

The aim of the present study was to assess the effects of Linomide on the angiogenic response that is induced when islets are implanted in the dorsal skinfold chamber of the hamster. The choice of islets of Langerhans as inducers of physiological, controlled angiogenesis in this model allows us to separate Linomides antiangiogenic effects from its antitumor effects and also provides us with a highly reproducible method that facilitates the evaluation of the antiangiogenic effects of Linomide. For elucidation of the dosage regimen, the pharmacokinetics of Linomide was studied.

Materials and methods

Animal model and surgical techniques. The dorsal skinfold chamber in the hamster has previously been described in detail [5]. In brief, male Syrian Golden hamsters (55–70 g) were anesthetized using sodium pentobarbital (Nembutal, 50 mg/kg, i.p.). Two symmetrical titanium frames were implanted into the dorsal skinfold so as to sandwich the extended double layer of skin. One layer of the skin was completely removed in a circular area measuring 15 mm in diameter. The underlaying thin layer of muscle (musculus cutaneous max.) and the subcutaneous tissue was covered with a coverslip incorporated in one of the frames. In addition, a permanent catheter was passed from the dorsal to the ventral side of the neck and inserted into the jugular vein.

Islet isolation and implantation. Islets of Langerhans were isolated after staining with neutral red by a modified collagenase technique [16], which allows the isolation of 500–800 islets from a hamster donor pancreas. A handpicking procedure guarantees that single exocrine-free islets of equal size (200–250 μm in diameter) are obtained for transplantation. At 2 days after implantation of the skinfold chambers, the transplantation of islets was performed by removing the coverslip and carefully placing about ten islets on the skeletal muscle within the chamber using a micro-pipette. One group of hamsters ($n = 9$) was force-fed Linomide twice a day starting at the day of transplantation of islets. Linomide was mixed with sterile water to a final concentration of 15 mg/ml and given so as to correspond to a dose of 100 mg/kg per day.

Intravital microscopy and analysis. Unanesthetized animals were immobilized in a plexiglass tube that was attached to the microscope stage (Leitz, Biomed). Fluorescence microscopy was performed using epi-illumination by a Leitz Ploemopak epi-illuminator equipped with an I2 filter block and video-triggered stroboscopic illumination from a xenon arc (Strobex 236; Chadwick Helmuth, Mountain View, Calif., USA). Observations were made using a Nikon X10 (numerical aperture, 0.30) and a Leitz X25 (numerical aperture, 0.60) objective. At the day of islet implantation, an overview video print (Sony Color Video Printer UP-3000) was taken using a Leitz PL 1.6X (numerical aperture, 0.05) objective, and the positions of the implanted islets were marked to facilitate the localization of islets at later observations. Observations were performed at 6, 10, and 14 days after the implantation of islets using i.v. injections of 0.2 ml 5% fluorescein isothiocyanate (FITC)-dextran 150,000 to obtain contrast enhancement. A silicon intensified target camera (SIT68; Dage-MTI, Michigan City, Ind., USA) was attached to the microscope and connected to a monitor (Panasonic TR-930) and the experiments were recorded using an S-VHS video cassette recorder (JVC HR-S6600 U) for off-line analysis of islet neovascularization. For each islet, the recording obtained using the Nikon X10 objective was examined to determine the area of angiogenesis. A second recording was made with the Leitz X25 objective, which was used to calculate functional capillary density, defined as the length of capillaries perfused with red blood cell per area of the islets. To obtain the total length of capillaries within a microvascular network of an islet, a transparency was put in front of the monitor and a drawing was made using a pen (Sanford, Sharpie Fine Point), with great care being taken to draw with the same line width for all vessel segments. Capillaries from all focal planes within the microvascular network were drawn on the same transparency. The transparency was scanned using a Hewlett-Packard Scanjet Plus scanner. The obtained image file was analyzed in terms of calculating the total number of black pixels in each file; assuming equal line width, this number would be proportional to the length of the vascular network. A calibration curve was constructed by making seven drawings of known lengths with the same pen. A linear regression curve was calculated to obtain the proportionality constant ($R^2 = 0.999$).

Pharmacokinetics of Linomide in hamsters. Seven groups of six male Syrian golden hamsters were given a single dose of 100 mg/kg Linomide. The dose was given in a water solution as 20 mg Linomide/ml water. Groups of animals were euthanized at 0.5, 1, 2, 4, 8, 12, and 24 h after dosing. The animals were anesthetized with sodium pentobarbital (Nembutal, 50 mg/kg, i.p.), and blood was immediately drawn by means of cardiac puncture and collected in heparinized tubes. Plasma was separated within 1 h by centrifugation (1300 *g*, +4° C, 15 min). The plasma samples were stored at −20° C until analysis. The elimination rate constant, β, was determined by linear regression analysis of the slope between 8 and 24 h of the logarithmic plasma concentration-time curve. The corresponding half-life, $t_{1/2\beta}$, was determined from its relationship to β: $t_{1/2\beta} = \ln 2/\beta$.

Plasma analysis of Linomide. Samples were spiked with a known amount of the chlorinated analogue of Linomide, used as an internal standard, and applied on a solid-phase extraction column (SEP-Pak C_{18} cartridge; Ters Associates, USA). The internal standard was synthesized at Pharmacia laboratories and characterized using nuclear magnetic resonance (NMR) and infrared (IR) spectra and elemental analysis. Samples with an expected high concentration of Linomide were diluted to volumes ranging from 0.100 to 5.00 ml prior to analysis. After a clean-up step, Linomide and the internal standard were eluted from the column with methanol; the elute was evaporated, redissolved in the mobile phase, and filtered; and 40 μl of the solution was injected into the chromatographic system. The separation was achieved on a reverse-phase column (Nova pak C_{18}; 15 cm × 3.9 mm; Waters Associates, USA) using a mixture of acetonitrile-water-1 M phosphoric acid (325+525+150) as a mobile phase. Linomide and the internal standard were detected by UV monitoring at 287 nm, and chromatograms were evaluated using a JCL 6000 Chromatography Data System (Jones Chromatography, England). The peak height ratio between the Linomide peak and the internal standard peak was used for evaluation. The detection limit and the quantification limit of the method were evaluated using the baseline noise on chromatograms derived from human blank plasma. The detection limit was estimated to be 0.02 μ*M* and the quantification limit, 0.065 μ*M*. The precision and accuracy of the assay was checked on every occasion of analysis. Human blank plasma with known amounts of Linomide added (0.25 and 2.5 nmol/ml) was analyzed in parallel with other samples. About 8% of all analyzed samples were these control samples. The precision of the determination expressed as the relative standard deviation was 3.0% for high-level samples and 6.3% for low-level samples. The recovery ranged between 100.7% and 102.2%.

Reagents. Linomide (*N*-phenylmethyl-1,2,dihydro-4-hydroxyl-1-methyl-2-oxoquinoline-3-carboxamide) is the registered trademark for Roquinimex (Pharmacia, Helsingborg, Sweden). Linomide was synthesized at Pharmacia. FITC-dextran 150,000, used for contrast enhancement, was obtained from Sigma (St. Louis, Mo., USA).

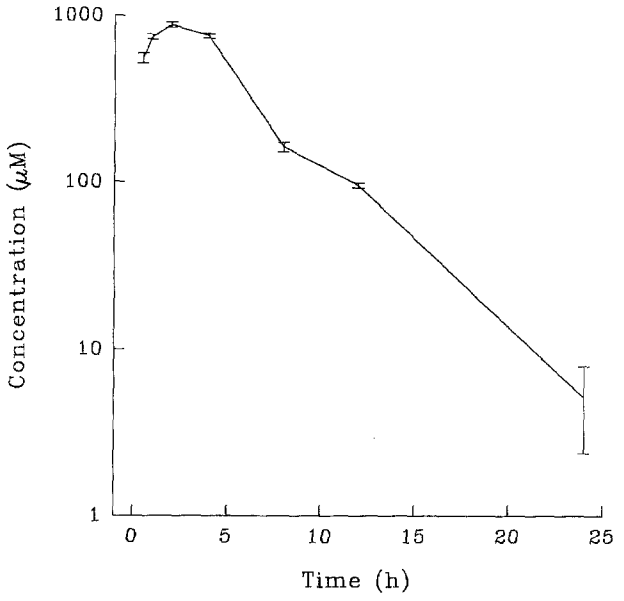

Fig. 1. Plasma concentration of Linomide (Roquinimex) following a single oral dose of the compound, 100 mg/kg, to male hamsters

Statistical analysis. The data were subjected to normality and equal variance tests, which revealed normal distribution, and the results are presented as the mean values ±SE. Statistical analysis was carried out using Students *t*-test (* $P<0.05$; ** $P<0.01$; *** $P<0.001$). The statistical calculations were computed with SigmaStat.

Results

The plasma concentration profile of Linomide following a single oral dose of 100 mg/kg is depicted in Fig. 1. The maximum plasma concentration, 875±90 μ*M* (mean ±SEM), was obtained at 2 h after administration. At 8 h after dosing, the plasma concentration had decreased 5-fold to 162±29 μ*M*. The elimination of Linomide was fast, the half-life being 2.6±0.2 h. Due to the short half-life, the hamsters were given Linomide twice a day.

Figure 2 illustrates the glomerulus-like microvascular networks typical of islet grafts in the dorsal skinfold of the hamster. These networks are very similar to those found for pancreatic islets in situ. The upper left-hand panel shows the vasculature of an islet from the control group as obtained with the Nikon X10 objective at 14 days after transplantation. The upper right-hand panel shows the same islet as recorded with the Leitz X25 objective. The lower left-hand

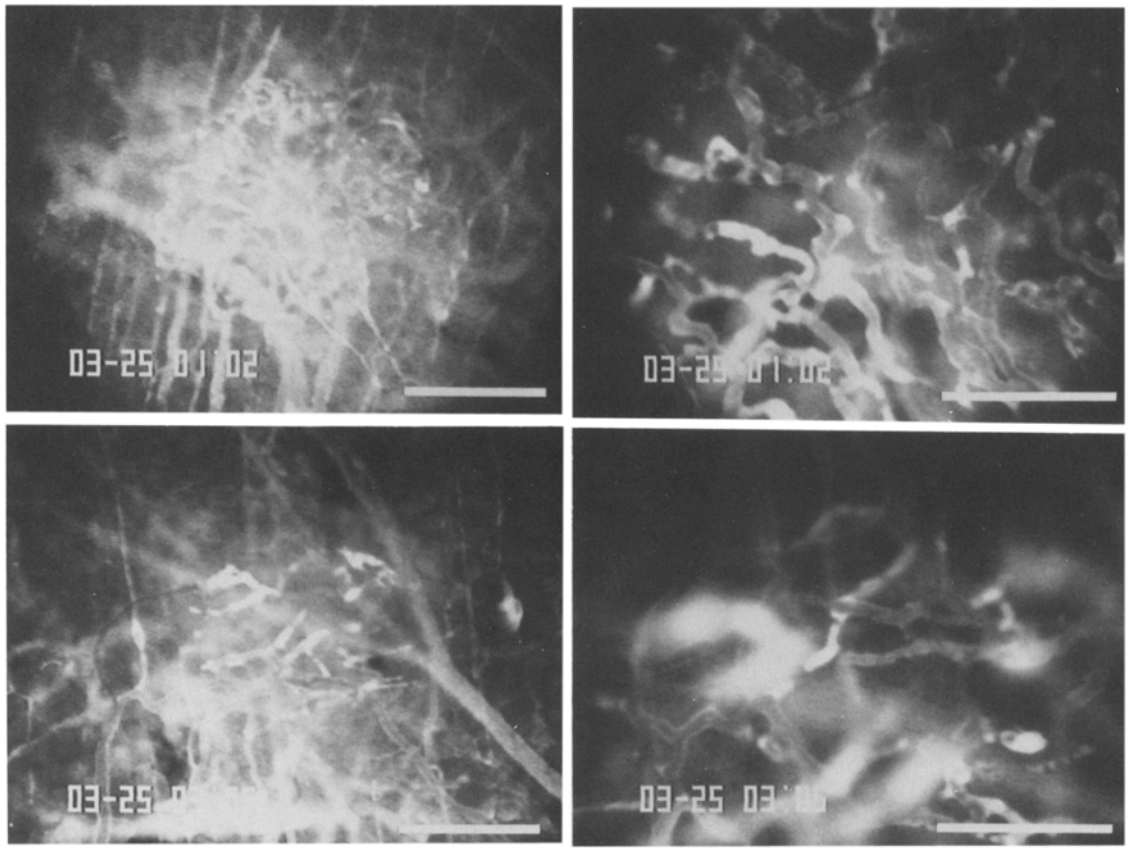

Fig. 2. Comparison of the microvasculature of pancreatic islet grafts in control versus Linomide-treated animals at 14 days after transplantation. The *upper panels* are from a control animal and the *lower panels* are from an animal treated with Linomide (100 mg/kg per day). Note the smaller network area and the lower capillary density in the Linomide-treated animal. Bars: *left-hand panels*, 200 μm; *right-hand panels*, 100 μm

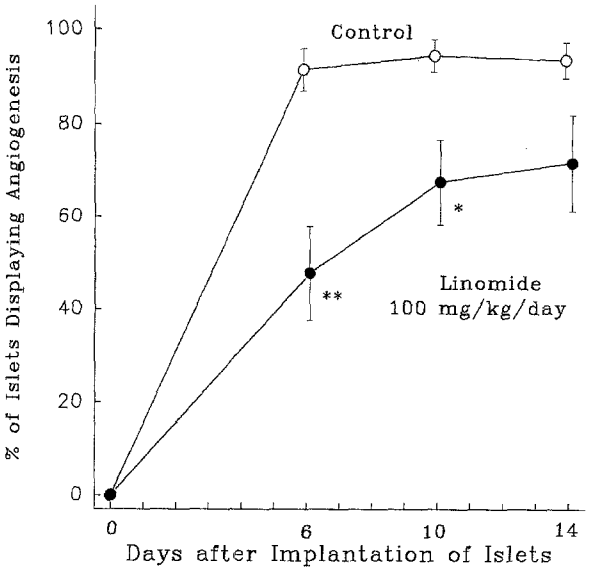

Fig. 3. Percentage of transplanted islets showing any sign of angiogenesis for the two groups at 6, 10, and 14 days after transplantation of the isletgrafts into the hamster dorsal skinfold chamber. * $P<0.05$; ** $P<0.01$; *** $P<0.001$ (Student t-test)

panel shows the vasculature of an islet from the group treated with Linomide (100 mg/kg per day) as obtained with the Nikon X10 objective, and the lower right-hand panel shows the same islet as recorded with the Leitz X25 objective. Contrast enhancement was obtained by means of i.v. injection of FITC-dextran 150,000.

The first signs of angiogenesis are dilated and tortuous capillaries in the skeletal muscle of the host tissue, protrusions of buds from the capillaries, and, often, also petechial hemorrhages. If an area where an islet was transplanted lacked such signs, the islet was considered not to display angiogenesis, and this so called "take-rate" was the first parameter to be quantified in the present study. The control group comprised 7 animals implanted with a total of 60 islets and the Linomide-treated group consisted of 9 animals implanted with 71 islets. Figure 3 depicts the take-rate recorded for the group of animals treated with Linomide as compared with the control group at 6, 10, and 14 days after transplantation. At day 6 after transplantation, 91% ± 4% of the control islets showed the first signs of angiogenesis, whereas new microvessel formation could be observed in only 48% ± 12% of the Linomide- treated grafts. At 10 days after transplantation, the take-rate in the Linomide-treated animals had increased to 67% ± 11% and that in the control group had risen to 94% ± 3%. At day 14, the take-rate in the treated group was 72% ± 12% ($n = 6$) and that in the control group was 94% ± 4% ($n = 6$). These differences were significant at days 6 and 10 but not at day 14.

A histogram depicting the relative occurrence of functional capillary density (FCD) for control animals (upper panels) and Linomide-treated animals (lower panels) at days 6, 10, and 14 is shown in Fig. 4. FCD is grouped in intervals of 50 cm^{-1}, and the dotted line in each panel illustrates the corresponding normal distribution. The Fig. illustrates the inhibitory effect of Linomide on islet-induced angiogenesis and revascularization, revealing that at day 6 after implantation, 58% of the islets in the Linomide-treated group had an FCD of less than 50 cm^{-1} as compared with 7% of those in the control group. At day 10, almost 40% of the islets in the Linomide-treated group had an FCD of less than 50 cm^{-1} as compared with less than 6% of those in the control group. Furthermore, at day 14, only 20% of the islets in the Linomide-treated group had an FCD of greater than 500 cm^{-1} as compared with 75% of those in the control group. In both groups, the mean FCD value increased with time, whereas the distribution became more homogeneous. However, the Linomide-treated group showed not only a lower mean value for but also a much wider distribution of FCD, with coefficients of variation being 3 times larger in these animals than in the control group on similar days.

Figure 5 shows the compiled data for FCD, with the vascular densities of islets being averaged within individual

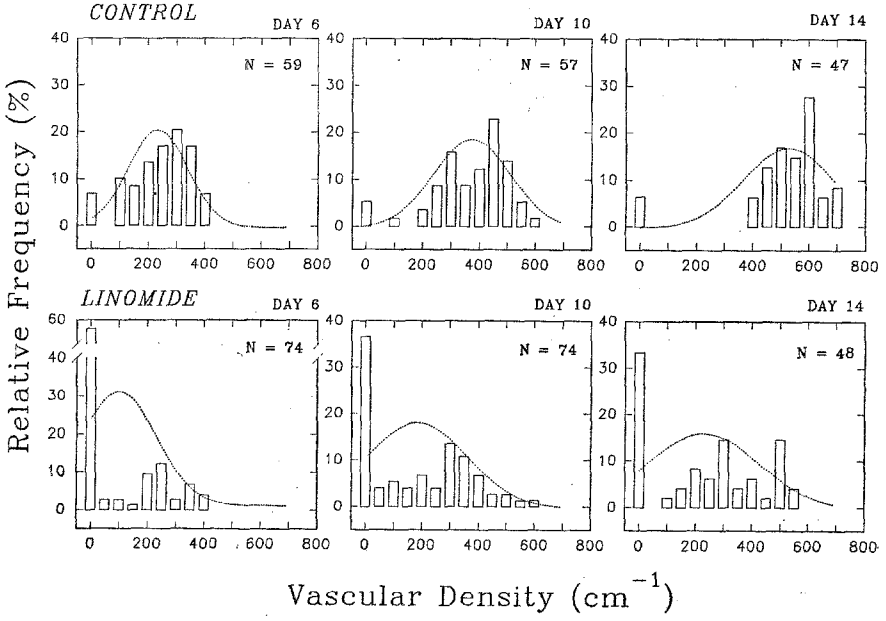

Fig. 4. Histogram depicting the relative occurrence of FCD for control animals (*upper panels*) and Linomide-treated animals (*lower panels*) at days 6, 10, and 14. FCD is grouped in intervals of 50 cm^{-1}, and the *dotted line* in each panel illustrates the corresponding normal distribution

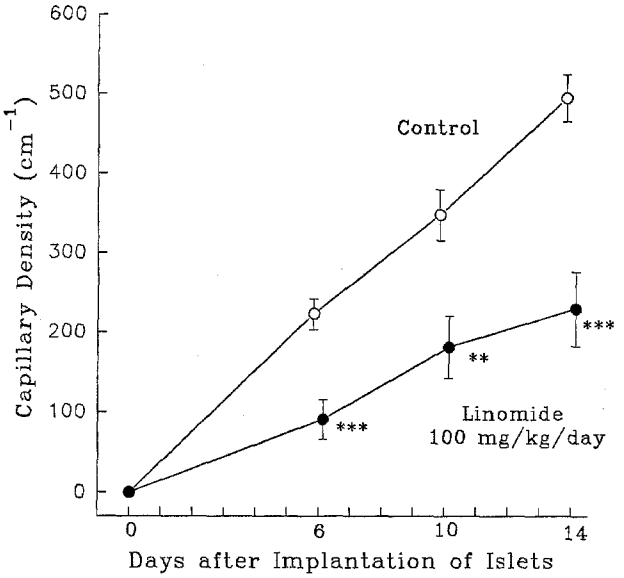

Fig. 5. FCD of pancreatic islet grafts at 6, 10, and 14 days after transplantation

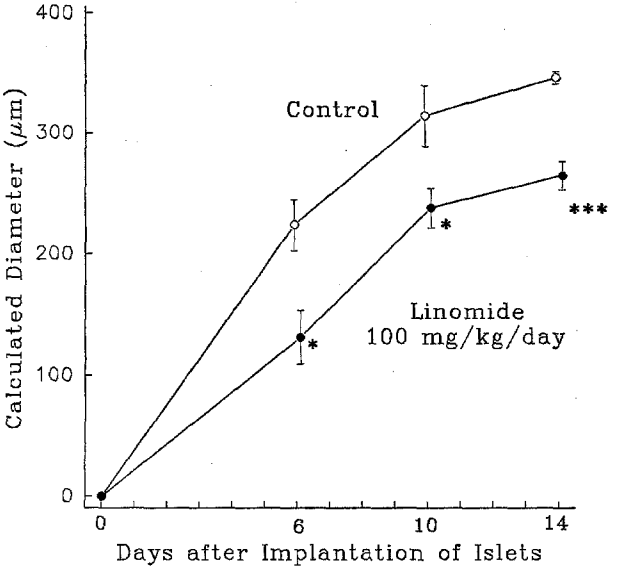

Fig. 6. Effect of Linomide on the "calculated" diameter of neovascularization. The area (A) of an islet showing signs of angiogenesis was used to obtain the "calculated" diameter (D_c) of the revascularized area according to the formula $D_c = 2\sqrt{A/\pi}$

animals. At days 6, 10, and 14, the FCD in the control group was 223 ± 17, 348 ± 29, and 495 ± 29 cm^{-1}, respectively, whereas that in the Linomide-treated animals was 91 ± 28, 181 ± 43, and 229 ± 47 cm^{-1}, respectively. This corresponds to a 59%, a 48%, and a 54% inhibition of the revascularization process at the respective time points, with all differences being statistically significant.

Although we did not measure the diameter of each islet prior to its implantation, the handpicking procedure allowed us to choose islets of the same size, which corresponded to islets with a diameter on the order of 200 – 250 μm. The area (A) of an islet showing signs of angiogenesis was used to obtain the "calculated" diameter (D_c) of the revascularized area according to the formula $D_c = 2\sqrt{A/\pi}$. Figure 6 shows the compiled D_c data for islets implanted in control animals and in animals treated with Linomide. At days 6, 10, and 14, the D_c in control animals was 224 ± 20, 314 ± 24, and 346 ± 6 μm, respectively, whereas that in animals treated with Linomide was 132 ± 27, 238 ± 20, and 265 ± 13 μm, respectively. All differences were statistically significant.

Discussion

Recent studies have suggested that in addition to being an immunomodulator, the quinoline-3-carboxamide Linomide also possesses antiangiogenic properties [13, 34]. However, direct evidence for the antiangiogenic effect of Linomide in vivo is lacking, perhaps partly because the effect of Linomide is seen only in vivo but not in vitro and because adequate models allowing direct in vivo analysis of angiogenesis are scarce.

The complex process of angiogenesis and the different steps involved in neovascularization have been studied in a variety of different in vitro models focusing on components of angiogenesis such as degradation of the basement membrane [9], migration [8], proliferation [6], and formation of three-dimensional capillary tubes [21]. However, at present only a few models are available for the study of angiogenesis in vivo. The most common is the cornea pocket model. In this model, angiogenesis is induced by the implantation in the eye of angiogenic factors embedded in a controlled-release polymer such as ethylene vinyl acetate or a cellulose disc [7, 22, 23]. The chorioallantoic membrane of the chick embryo [2] has also been used to study the sprouting of new vessels toward a pellet. Furthermore, alginate-encapsulated tumor cells [25, 26] and gelatin-impregnated sponges have been used as inducers of angiogenesis [33]. Recently, an in vivo assay allowing quantitative testing of angiogenic activity was developed by Passaniti et al. [24]. In this assay an extract of basement membrane (Matrigel) mixed with basic fibroblast growth factor (FGF) and heparin was used to induce angiogenesis.

Despite the multitude of experimental model systems available for the study of angiogenesis, there is no system that allows reliable dynamic repetitive quantification of early angiogenesis in vivo. For many years, chambers implanted in various animal species have been used in combination with intravital microscopy to study microcirculatory phenomena in situ [1, 3, 4, 12, 27–29]. In 1980, a dorsal chamber technique was developed in the hamster by Endrich et al. [5] and the technique was later utilized to investigate the revascularization of syngeneic transplants of islets of Langerhans [19]. In this model system, the revascularization process was found to be very reproducible, with almost 100% of transplanted islets showing signs of angiogenesis within 2–4 days and most islets being fully vascularized within 10 days. The above mentioned technique was originally designed for the study of rejection phenomena, but due to its high reproducibility and excellent resolution, we decided to implement this technique to study for the first time the proposed antiangiogenic effects of Linomide on normal angiogenesis in vivo. Due to the lack of

detailed information regarding the exact mechanisms underlying islet-induced angiogenesis as compared with those underlying tumor-induced angiogenesis and since the antiangiogenic properties of Linomide are of interest in relationship to its antitumor effect, our choice of islets of Langerhans could be criticized. However, since islet-induced angiogenesis (a) is extremely reproducible [18], facilitating the evaluation of the antiangiogenic effects of Linomide, and (b) is a physiological, well-controlled process as opposed to tumor-induced angiogenesis, allowing us to differentiate between direct antitumor effects and antiangiogenic effects, we consider islets of Langerhans to be an excellent choice as an inducer of angiogenesis.

In earlier studies using the same model system with syngeneic implants of islets of Langerhans, it was reported that 97% [18] and 100% [20] of transplanted islets were fully vascularized within 10 days. In the present study, 94% of the implanted islets in the control group were vascularized at day 10. However, at 10 days after implantation, our islets displayed a capillary density of 350 cm^{-1}, whereas in the study of Menger et al. [20], islets had twice this capillary density at the corresponding time point. At day 14, the capillary density of our islets had increased to almost 500 cm^{-1} as compared with the value of 700 cm^{-1} reported by Menger et al. [20].

Almost all islets that eventually displayed angiogenesis in the control group did so within 6 days. In contrast, in Linomide-treated animals, only 48% of islets showed signs of angiogenesis at day 6; however, of the islets that did not display angiogenesis at day 6, 37% showed signs at day 10. Between day 10 and day 14, an additional 15% of islets that had not previously displayed angiogenesis started to do so. Since periods of observation longer than 14 days are difficult to accomplish, the occurrence of subsequent delayed angiogenesis in the remaining 28% of islets could not be assessed. The appearance, at 10 days in the Linomide-treated group, of new capillaries in islets that had not previously shown vascularization shows that islets are capable of surviving for at least 10 days in the skinfold chamber. This finding suggests that although Linomide has no direct cytotoxic effect on islets of Langerhans, it affects the initiation as well as the growth rate of the neovasculature.

Since Linomide profoundly affected the "take-rate" of islets (see Fig. 3), we decided to include islets that failed to show signs of angiogenesis throughout the 2-week observation period in the analysis of FCD. However, if we exclude the islets in both groups that did not show any sign of angiogenesis at day 14, the FCD value is nonetheless 47%, 34%, and 40% lower at day 6, day 10, and day 14, respectively, in the Linomide-treated group, indicating that Linomide also affects the proliferation rate of endothelial cells. From Fig. 5 it can be seen that the rate of change in FCD was about 50% lower in the Linomide-treated animals as compared with the control group. The magnitude of inhibition corresponds well with results obtained earlier with the Matrigel in vivo angiogenesis assay in rats [34], where a 41% inhibition of capillary density at a Linomide dose of 100 mg/kg per day was found.

In conclusion, we find that Linomide (100 mg/kg per day) inhibits angiogenesis induced by islets of Langerhans in the skinfold chamber of the hamster by (a) decreasing the number of islets displaying angiogenesis, (b) delaying the onset of angiogenesis, (c) decreasing the growth rate of capillaries by more than 50%, (d) reducing the area of neovascularization by 25%, and, hence, (e) reducing the total proliferation of endothelial cells by more than 60%.

References

1. Arfors K-E, Johnsson JA, McKenzie FN (1970) A titanium rabbit ear chamber: assembly, insertion, and results. Microvasc Res 2: 516–519
2. Ausprunk DH, Knighton DR, Folkman J (1975) Vascularization of normal and neoplastic tissues grafted to the chick chorioallantois: role of host and pre-existing graft blood vessels. Am J Pathol 79: 597
3. Clark EE, Kirby-Smith HT, Rex RO, Williams RG (1930) Recent modifications in the method of studying living cells and tissues in transparent chambers inserted in the rabbit's ear. Anat Rec 47: 187–211
4. Endrich B, Intaglietta M, Reinhold HS, Gross JF (1979) Hemodynamic characteristics in microcirculatory blood channels during early tumor growth. Cancer Res 39: 17–23
5. Endrich B, Asaishi K, Goetz A, Messmer K (1980) Technical report – a new chamber for microvascular studies in unanesthetized hamsters. Res Exp Med 177: 125–134
6. Gimbrone MA Jr, Cotran RS, Folkman J (1973) Endothelial regeneration and turn-over. Studies with human endothelial cell cultures. Ser Haematol 6: 453
7. Gimbrone MA, Cotran RS, Leapman SB, Folkman J (1974) Tumor growth and neovascularization: an experimental model using the rabbit cornea. J Natl Cancer Inst 52: 413
8. Glaser BM, D'Amore PA, Sepa H, Seppa S, Schiffmann E (1980) Adult tissues contain chemoattractants for vascular endothelial cells. Nature 288: 483
9. Gross JL, Moscatelli D, Rifkin DB (1983) Increased capillary endothelial cell protease activity in response to angiogenic stimuli in vitro. Proc Natl Acad Sci USA 80: 2623
10. Harning R, Szalay J (1988) A treatment of murine ocular melanoma. Invest Ophthalmol Vis Sci 29: 1505–1510
11. Harning R, Koo GC, Szalay J (1989) Regulation of metastasis of murine ocular melanoma by natural killer cells. Invest Ophthalmol Vis Sci 30: 1909–1915
12. Hobbs JB, Chusilp S, Hua A, Kincaid-Smith P, McIver MA (1976) The pathogenesis of hypertensive vascular changes in the rat: microscopic and ultrastructural correlation in vivo. Clin Sci 51: 71–75
13. Ichikawa T, Lamb JC, Christensson PJ, Hartley-Asp B, Isaacs JT (1992) The antitumor effects of the quinoline-3-carboxamide linomide on dunning R-3327 rat prostatic cancers. Cancer Res 52: 3022–3028
14. Kalland, T (1986) Effects of immunomodulator LS-2616 on growth and metastasis of the murine B16-F10 melanoma. Cancer Res 46: 3018–3022
15. Kalland T, Alm G, Stålhandske T (1985) Augmentation of mouse natural killer activity by LS-2616, a new immunomodulator. J Immunol 134: 3956–3961
16. Lacy PE, Kostianovsky M (1967) Method for the isolation of intact islets of Langerhans from rat pancreas. Diabetes 16: 35–39
17. Larsson E-L, Joki A, Stålhandske T (1987) Mechanism of action of the new immunomodulator LS-2616 on T-cell responses. Int J Immunopharmacol 9: 425–431
18. Menger MD, Jaeger S, Walter P, Feifel G, Hammersen F, Messmer K (1989) Angiogenesis and hemodynamics of the microvasculature of transplanted islets of Langerhans. Diabetes 38 [Suppl 1]: 199–210
19. Menger MD, Jäger S, Walter P, Hammersen F, Messmer K (1990) A novel technique for studies of the microvasculature of trans-

planted islets of Langerhans in vivo. Int J Microcirc Clin Exp 9: 103–117
20. Menger MD, Wolf B, Höbel B, Shorlemmer H-U, Messmer K (1991) Microvascular phenomena during pancreatic islet graft rejection. Langenbecks Arch Chir 376: 214–221
21. Montesano R, Orci L (1985) Tumor-promoting phorbol esters induce angiogenesis in vitro. Cell 42: 469
22. Moses MA, Langer R (1991) Inhibitors of angiogenesis. Biotechnology 9: 630–634
23. Muthukaruppan VR, Auerbach R (1979) Angiogenesis in the mouse cornea. Science 205: 1416
24. Passaniti A, Taylor RM, Gage WR, Pili R, Guo Y, Long PV, Haney JA, Pauly RR, Grant DS, Martin GR (1992) A simple, quantitative method for assessing angiogenesis and antiangiogenic agents using reconstituted basement membrane, heparin and FGF. Lab Invest 67: 519–528
25. Plunkett ML, Hailey JA (1990) An in vivo quantitative angiogenesis model using tumor cells entrapped in alginate. Lab Invest 62: 510–517
26. Robertson NE, Discafani CM, Downs EC, Hailey JA, Sarre O, Runkle RL, Popper TL, Plunkett ML (1991) A quantitative in vivo mouse model used to assay inhibitors of tumor-induced angiogenesis. Cancer Res 51: 1339–1344
27. Rutili G, Arfors K-E (1976) Technical report: fluorescein-labelled dextran measurement in interstitial fluid in studies of macromolecular permeability. Microvasc Res 12: 59–70
28. Greenblatt M, Shubik P (1967) Hamster cheekpouch chamber. Cancer Bull 19: 65–81
29. Sandison JC (1928) The transparent chamber of the rabbit's ear giving a complete description of improved techniques of construction and introduction and general account of growth and behavior of living cells and tissues as seen with the microscope. Am J Anat 41: 447–472
30. Stålhandske T, Kalland T (1986) Effects of the novel immunomodulator LS-2616 on the delayed-type hypersensitivity reaction to *Bordetella pertussis* in the rat. Immunopharmacology 11: 87–92
31. Stålhandske T, Eriksson E, Sandberg B-M (1982) A novel quinolinecarboxamide with interesting immunomodulatory activity. Int J Immunopharmacol 4: 336–341
32. Tarkowski A, Gunnarson K, Nilsson L-Å, Lindholm L, Stålhandske T (1986) Successful treatment of autoimmunity in MRL/l. mice with LS-2616, a new immunomodulator. Arthritis Rheum 29: 1405–1409
33. Thompson JA, Anderson KD, DiPietro JM, Zwiebel JA, Zametta M, Anderson WF, Maciag T (1988) Site-directed neovessel formation in vivo. Science 241: 1349–1352
34. Vukanovic J, Passaniti A, Hirata T, Traystman RJ, Hartley-Asp B, Isaacs JT (1993) Antiangiogenic effects of the quinoline-3-carboxamide, Linomide. Cancer Res 53: 1833–1837